# A Digital, Constant-Frequency Pulsed Phase-Locked-Loop Instrument for Real-Time, Absolute Ultrasonic Phase Measurements

Harold A. Haldren and Mool C. Gupta
*University of Virginia, Charles L. Brown Department of Electrical and Computer Engineering, Thornton Hall, 351 McCormick Rd, Charlottesville, VA 22904*

Daniel F. Perey, William T. Yost, and K. Elliott Cramer
*NASA Langley Research Center, 4 Langley Blvd, Bldg. 1230, MS 231, Hampton, VA 23681*

A digitally-controlled instrument for conducting single-frequency and swept-frequency ultrasonic phase measurements has been developed based on a constant-frequency pulsed phase-locked-loop (CFPPLL) design. This instrument uses a pair of direct digital synthesizers to generate an ultrasonically-transceived tone-burst and an internal reference wave for phase comparison. Real-time, constant-frequency phase tracking in an interrogated specimen is possible with a resolution of 0.00038 radians (0.022°), and swept-frequency phase measurements can be obtained. Using phase measurements, absolute thickness in borosilicate glass is presented to show the instrument's efficacy, and these results are compared to conventional ultrasonic pulse-echo time-of-flight (ToF) measurements. The newly-developed instrument predicted thickness with a mean error of -0.04 μm and a standard deviation of error of 1.35 μm. By showing higher accuracy and precision than conventional pulse-echo ToF measurements, the new digitally-controlled CFPPLL instrument provides high-resolution absolute ultrasonic velocity or path-length measurements in solids or liquids, as well as tracking of material property changes with high sensitivity. In addition to improved resolution, swept-frequency phase measurements add useful capability in measuring properties of layered structures, such as bonded joints, or materials which exhibit non-linear frequency-dependent behavior, such as dispersive media.

## I. INTRODUCTION

Ultrasonic phase measurements have been used for many years to measure absolute and relative material properties. The phase, rather than amplitude, of ultrasonic waves is ideally-suited for these measurements due to its sensitivity to the wavelength and thickness of a material specimen. Methods of accurately determining the time delay between received ultrasonic echoes date back as far as the 1960s with the pulse-superposition method by McSkimin [1] and the pulse-echo-overlap method by Papadakis [2]. Several improvements to broadband time-domain ultrasonic velocity-change measurements with damped transducers have been made throughout the years [3], [4]. Other pulse-echo methods involve finding the resonance frequency of the material [5], [6] or utilize continuous-wave sources to introduce standing waves rather than broadband sources [7].

For high-accuracy measurements, single frequency gated continuous wave (tone-burst) ultrasonic techniques increase the signal-to-noise ratio of their broadband counterparts. By comparing a received ultrasonic wave signal with a reference signal and adjusting the driving frequency until the waves are in quadrature ($\pi/2$ phase difference), a highly-sensitive measurement of changes in

sound velocity or material thickness is obtained [8]. The phase comparison technique has since spawned several variations of pulsed phase-locked loop (PPLL) ultrasonic phase measurement methods.

The initial variable-frequency PPLL systems were used in applications of bolt tension monitoring [9] , as well as detecting changes in sound velocity [10]. A major drawback of variable-frequency phase measurement methods is their sensitivity to frequency-dependent sources of phase error in the instrumentation electronics, transducers, and material. Furthermore, variable-frequency methods are unable to measure true phase changes within a specimen, as they rely on changing frequency to make a single-phase measurement. Consequently, the constant-frequency PPLL (CFPPLL) provides a major improvement for conducting ultrasonic phase measurements [10].

The original CFPPLL design utilized a single driving frequency, a voltage-controlled phase shifter, and a phase detector to lock the transmitted and reference waves in quadrature [11]. This instrument measured absolute phase velocities in liquids by tracking the phase shift induced when changing the ultrasonic path length; however, only changes in ultrasonic velocity due to external stimuli, such as pressure or temperature, were measurable in solids. Nonetheless, in comparison to the variable frequency PPLL counterpart, the CFPPLL provided very high accuracy and sensitivity.

A digitally-controlled CFPPLL instrument capable of real-time ultrasonic tracking of phase and swept-frequency phase measurements on both solids and liquids is explored. This instrument offers significant improvements in ease-of-use due to digital control and data collection capabilities. Whereas previous PPLL-based instruments required the changing of path-length to conduct absolute sound velocity measurements in liquids, both constant-frequency phase tracking and phase vs. frequency measurements of this CFPPLL instrument permit other experimental approaches. To illustrate this flexibility, experimental measurements of small differences in path-length in borosilicate glass via the CFPPLL instrument are shown and compared with conventional pulse-echo time-of-flight (ToF) measurements for thickness measurement accuracy and precision.

## II. THE DIGITALLY-CONTROLLED CONSTANT FREQUENCY PULSED PHASE-LOCKED LOOP

All PPLL devices consist of two signal paths along which the first, an ultrasonically transceived tone-burst, is phase-compared to a reference wave. On Path 1, the transducer generates an ultrasonic tone-burst which traverses a material specimen. In a pulse-echo arrangement, the same transducer receives and converts the tone-burst back into an electrical signal, while in a pitch-catch arrangement, a second transducer is used to receive the tone-burst. On Path 2, the reference wave is phase-compared to the transceived tone-burst from the first path. In a variable-frequency PPLL, the frequency of the transceived tone-burst is varied until the signals are in quadrature, while in a CFPPLL, the relative phase of the transceived signal is changed. The system is then considered to be in a locked state, and quadrature is maintained through continual updates to frequency or relative phase of the transceived signal.

In the digitally-controlled CFPPLL instrument, a pair of direct digital synthesizers (DDSs) generate sine waves with a repeatable constant phase offset, permitting absolute ultrasonic phase

measurements. While the system is in a locked state, the voltage output of a phase-detector is sampled by a microcontroller, which commands the DDS to adjust the transceived tone-burst's phase to maintain quadrature with the reference wave. A field-programmable gate array (FPGA) controls timing parameters and gating within the system.

A block diagram of the developed CFPPLL-based ultrasonic phase measurement instrument is shown in FIG. 1. Using a computer terminal, the user adjusts waveform and system parameters such as sample-and-hold (S/H) position, number of tone-burst cycles, repetition rate of the tone-burst, and number of sampled data points to average when taking phase measurements. After initial setup, the user locks the system which outputs the phase adjustments to the computer.

The twin DDSs generate sine waves at the frequency, amplitude, and phase set by the microcontroller. The same 1 GHz input timing clock is used for both DDSs, and upon system startup, the microcontroller synchronizes their output via a simultaneous reset command. The DDSs use lookup tables to generate the frequency and phase of the ultrasonic waves, which provide absolute frequency and phase adjustment resolution limits. The DDSs have 14 bits of phase resolution and 48 bits of frequency resolution, resulting in a minimum phase shift of ~0.00038 rad (0.022°) and a minimum frequency shift of ~3.55 μHz. Based on the timing information set by the microcontroller, the FPGA uses a transmit enable (TX EN) signal to gate the transceived wave in Path 1, forming a tone-burst of a set number of cycles.

The tone-burst in Path 1 is amplified and sent to a transducer, which ultrasonically interrogates a material specimen through a coupling medium. After being reflected off the back wall of the test specimen, the acoustic tone-burst is received by the same transducer in the pulse-echo setup, as shown in FIG. 1. Material property variations due to external stimuli such as pressure, temperature, elasticity, or path length are then detectable via ultrasonic phase shifts. After receiving the ultrasonic reflection, the transducer converts the tone-burst into an electrical signal. The FPGA timing ensures signals are continuously received using a receive enable (RX EN) signal, except for the short duration during tone-burst transmission.

The received tone-burst is amplified and band-pass filtered to reduce signal noise, and the reference wave passes through an identically-designed band-pass filter. Currently, the instrument operates with center frequency around 10 MHz, and the band-pass filtering circuits were both measured to have a -6 dB pass-band of 8.8-11.0 MHz. In practice, commercial damped transducers have displayed wider bandwidths than the band-pass filtering circuits, providing a minimal change to system bandwidth but providing a measurable phase response which must be characterized for high accuracy phase measurements.

After filtering, the received and reference signals pass into the phase detector. The phase detector outputs a voltage dependent on the phase difference between the two signals, using $\pi/2$ offset at the 0 V reference. The output voltage is low-pass filtered to minimize non-DC noise and is subsequently sampled and held using an analog-to-digital converter (ADC), whose output passes into the microcontroller. The S/H position on the received phase detector output signal is set by the FPGA and is user-specified. Each time the phase output is received by the microcontroller, the voltage output of a temperature probe which is typically adhered to the material test specimen is also sampled.

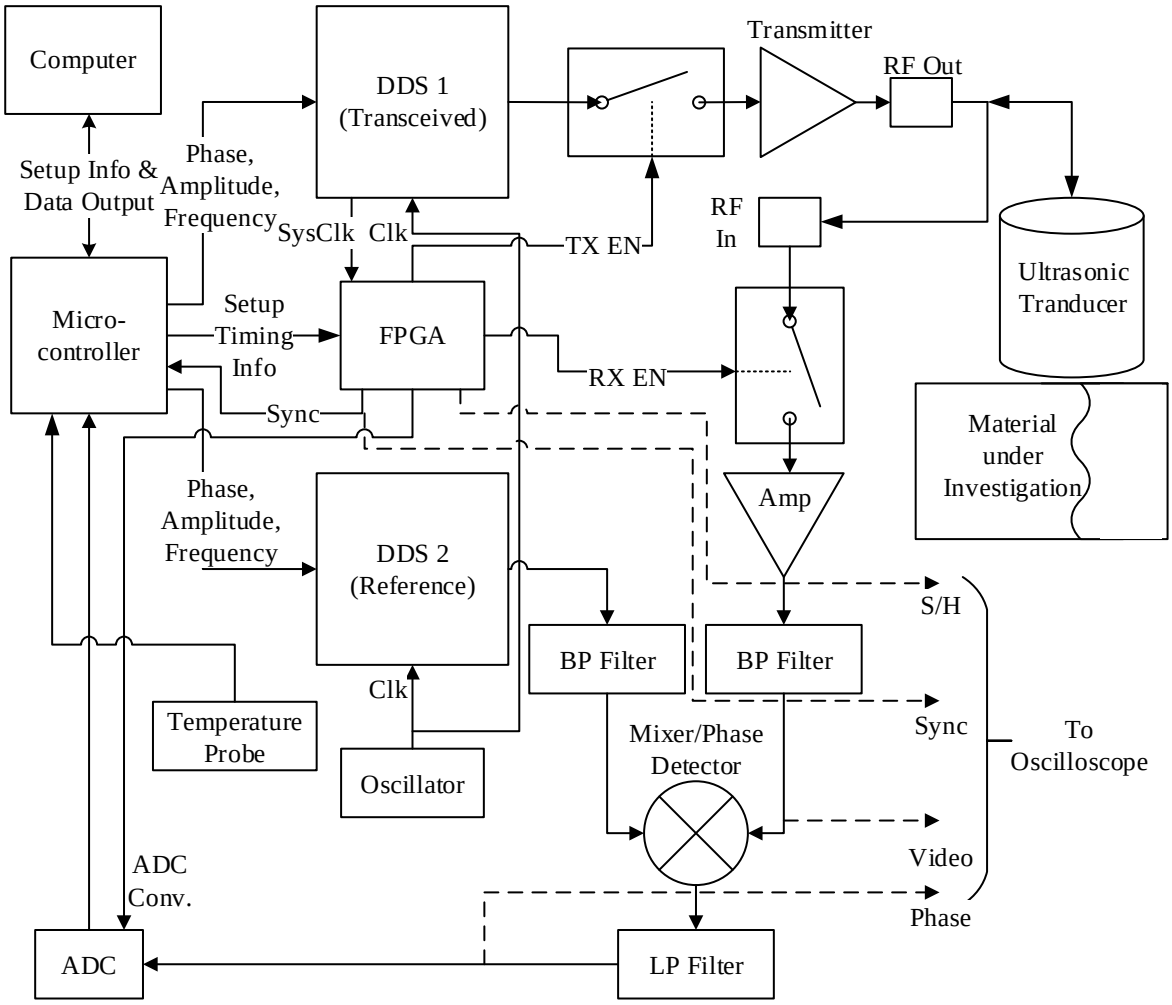


FIG. 1. Block diagram of digitally-controlled CFPPLL instrument

To properly monitor the system, the SYNC and S/H pulses from the FPGA, the amplitude of the transceived tone-burst after band-pass filtering, and the phase detector output voltage are all viewed on an oscilloscope. FIG. 2 shows an example of the oscilloscope CFPPLL signal display. The SYNC signal represents the beginning of each tone-burst transmission and is the trigger for the oscilloscope. The filtered amplitude signal, or video signal in FIG. 1, is used to observe ultrasonic reflections and helps the user determine waveform parameters. Often, the number of transmitted cycles is chosen to minimize the gap between successive reflections without overlapping. The phase and S/H signals are used to set the S/H position, typically in the portion of the received tone-burst where the phase appears flat. It should be noted there is a slight time delay between the video amplitude signal and the output of the phase detector; thus, the S/H position occurs slightly earlier than it appears on the amplitude signal.

The “bleed-thru” portion of the waveform is never actually transceived ultrasonically, but instead stays within the circuit. While the RX EN signal is off during the transmission period, some small amplitude leaks through and is amplified like the received ultrasonic reflections. It was first thought that this “bleed-thru” signal was undesirable; however, it has since proved useful in measuring the phase response of the filtering circuits.

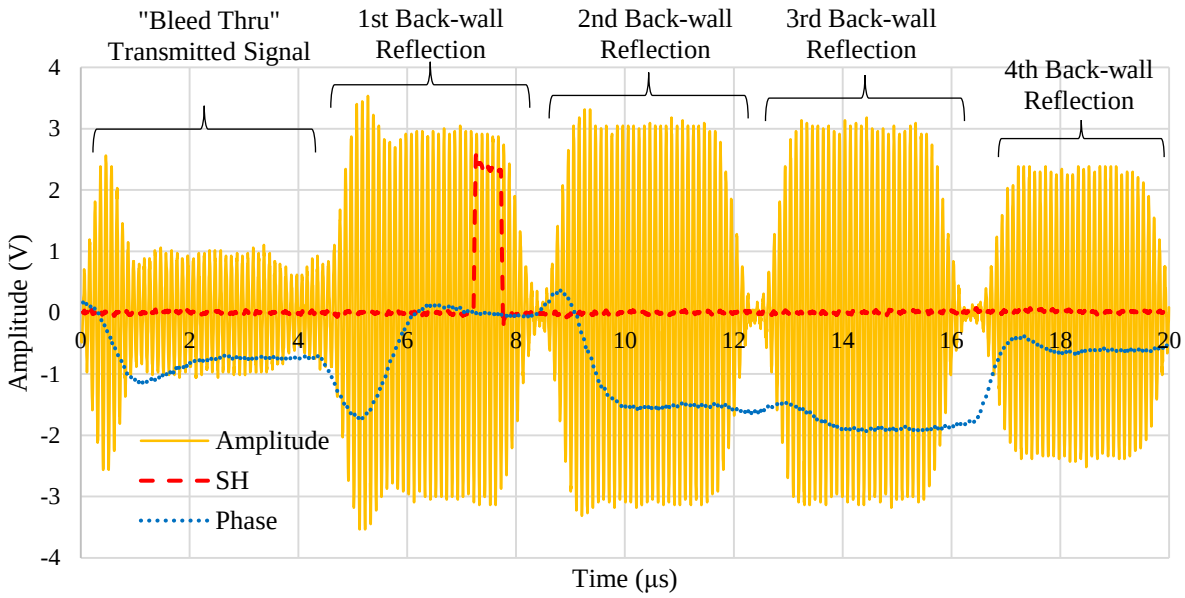


FIG. 2. Typical waveforms of received ultrasonic wave amplitude, phase detector output, and sample and hold (S/H) signals seen on oscilloscope when using CFPPLL instrument

## III. THICKNESS MEASUREMENT IN SOLIDS

### A. Theory

Assume an ultrasonic displacement plane wave is propagating within a non-dispersive medium of finite thickness, Medium 1. After reflection off the boundary with some half-space, Medium 2, and being received, as shown in FIG. 3, the phase of the ultrasonic wave is expressed as

$$\phi_{u_R} = -2k_1L_1 = -\frac{720fL_1}{c_1}\ [deg], \quad (1)$$

where $k_1 = \omega/c_1$ is the wavenumber in Medium 1 with sound velocity $c_1$, $\omega = 2\pi f\ [rad] = 360f\ [deg]$ is the driving angular frequency with driving frequency $f$, and $L_1$ is the thickness of Medium 1. The factor of two occurs due to the propagation through the thickness of Medium 1 twice. It is assumed in Equation 1 that the acoustic impedance of Medium 1 is greater than in Medium 2 or else the reflected wave would be $\pi$ out of phase with the incident wave.

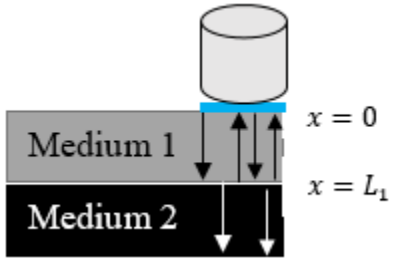


FIG. 3. Representation of ultrasonic wave reflections at boundary between Medium 1/Medium 2 and couplant layer

### a.) Swept-Frequency Phase Measurements

The phase of the reflected wave is used to measure either sound velocity or thickness of a material, given the other parameter. In non-dispersive media, the group velocity, $c_g = d\omega/dk$, is equal to the phase velocity, $c_p = dx/dt$ [10]. Thus, single-frequency phase measurements can find group velocity as well as phase velocity in non-dispersive media.

As constant-frequency phase measures relative fractions of a wavelength, expressed between $-\pi$ and $\pi$, it is difficult to obtain absolute thickness or sound velocity measurements since the total number of propagating wavelengths is unknown. Previous PPLL-based methods could measure absolute sound velocity in fluid media, where the acoustic path length was varied and $\partial\phi_{u_R}/\partial L_1$ measured [10], [11]. In solid media, only changes in sound velocity could be measured as path length could not be changed.

With the digitally-controlled CFPPLL instrument, the ultrasonic driving frequency can be altered while maintaining the phase relationship between the transceived and reference signals, allowing a measurement of $\phi_{u_R}(f)$. By sweeping the driving frequency and measuring the phase response, the sound velocity or specimen thickness is extracted by the relation,

$$\frac{\partial\phi_{u_R}}{\partial f} = -\frac{720L_1}{c_1}\left[\frac{deg}{Hz}\right]. \quad (2)$$

### b.) Pulse-echo Time-of-Flight Measurements

Traditional pulse-echo ultrasound can measure sound velocity or material thickness given knowledge of one of the parameters. After sending a broadband ultrasonic pulse through a material, the time-of-flight (ToF) of the received pulse is measured. Given the material setup in FIG. 3, the ToF for reflected waves is found by substituting the relation between time delay and phase, $\Delta t = \phi/\omega$, into Equation 1 to find

$$ToF = -\frac{2L_1}{c_1}\,[s]. \quad (3)$$

As the ToF does not suffer from a limited range of possible values like a constant-frequency phase measurement, a single ToF value can be used to measure sound velocity or specimen thickness.

### c.) Reducing Other Phase Shifts/Time Delays

In a practical direct-contact ultrasonic measurement system, the electronic circuitry, ultrasonic transducer, and ultrasonic couplant layer provide time delays or phase shifts. To avoid these errors, different methods are used to reduce or negate their effect. In conventional pulse-echo ToF measurements, a primary method for negating external time delays is to measure the ToF difference between successive back-wall echoes from a material. Delays due to the instrumentation, transducer, and double-transmission through the couplant layer affect successive echoes in the same way, so subtracting successive echoes will remove the circuit-based time-delays.

This technique can also be applied to constant-frequency phase measurements. Considering external phase shift sources for ultrasonic echoes from the material system, the measured phase for the $n^{th}$ echo can be described by

$$\phi_n = \phi_{instr.} + \phi_{trans.} + 2\phi_{coup.T} + 2\phi_{U_R} + (n-1)\left(2\phi_{U_R} + \phi_{coup.R}\right), \quad (4)$$

where $\phi_{instr.}$ is the phase shift from the instrumentation, $\phi_{trans.}$ is the phase shift from the ultrasonic transducer, $\phi_{coup.T}$ is the phase shift from transmission through couplant layer, $\phi_{coup.R}$ is the phase shift from reflection off the couplant layer occurring for secondary echoes, and $\phi_{U_R}$ is the phase shift from the material under investigation as defined in Equation 1. The phase difference between consecutive reflections from Equation 4 can be written as

$$\Delta\phi = \phi_{n+1} - \phi_n = 2\phi_{U_R} + \phi_{coup.R}, \quad (5)$$

where several of the external phase shift sources have been eliminated.

Remaining in Equation 5 is the phase shift of the reflection from the test material-couplant-transducer interface. There have been several treatments of the effect of the couplant layer on both the amplitude [12] [13] [14] [15] and time-delay [16] on an ultrasonic wave. If using a bare-element piezoelectric transducer, the effect of the couplant layer on the reflected phase can be derived given the material properties of the active element, couplant, and material under test. Commercially-available broadband ultrasonic transducers, however, contain additional layers which complicate analysis [16]. Furthermore, the internal setup of commercial transducers is often proprietary, which makes analysis of the ultrasonic reflection coefficient difficult without many assumptions.

Despite difficulties with calculating the actual reflection coefficient from the couplant interface, it can be shown that as the couplant becomes thinner, its effect on ultrasonic amplitude and phase lessens. By assuming a thin fluid layer between two half-spaces, the effect of a thin couplant layer can be approximated [17]. Assuming a PZT5A transducer, water couplant, and borosilicate glass specimen, the phase of the ultrasonic reflection coefficient as a function of frequency for different couplant thicknesses is shown in FIG. 4. The difference from the 180° phase shift for an infinitely thin couplant layer becomes more pronounced as the couplant layer thickness becomes larger with respect to wavelength. As the phase shift can vary dramatically for small differences in thickness, care must be taken to ensure a consistent couplant thickness to obtain high repeatability.

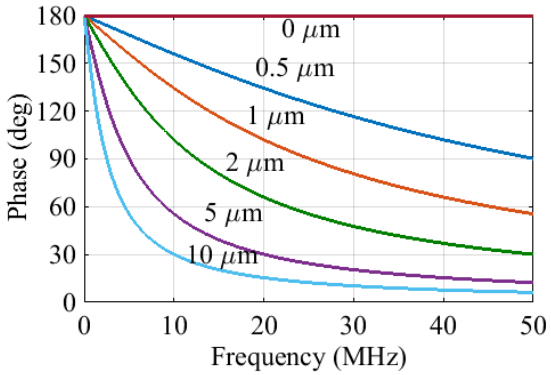

FIG. 4. Phase vs. Frequency of ultrasonic reflection off of couplant interface for different couplant thicknesses

## B. Experimental

To demonstrate the capabilities of the CFPPLL-based ultrasonic phase measurement instrument, measurements of micrometer-scale thickness differences in ~11 mm thick smooth glass specimens were performed. Six 5.08 cm x 5.08 cm square specimens were cut from a plate of Schott Borofloat® 33, a float-glass version of borosilicate glass, purchased from the S. I. Howard Glass Company. The specimens were cleaned in an ultrasonic bath of ethanol for 30 minutes prior to testing. Next, a 3 x 3 grid was marked off on each specimen using thin strips of tape to be used for thickness measurements.

At each of the nine locations on the six test specimens, the thickness was measured using a calibrated Starrett micrometer. The micrometer was calibrated by using Starrett-Webber gage blocks in the thickness range of interest, 10.9-11.0 mm, at every 1 μm. After correction, the micrometer measurements in the given range had a standard deviation of error of 1.05 μm.

To maintain consistent couplant layer thickness between measurements, a screw clamp was used to hold constant pressure and a load cell was placed in the path between the clamp and ultrasonic transducer. An experiment was performed to vary the pressure on the transducer while measuring the resulting phase shift of reflection from the back-wall of one of the glass specimens.

Another experiment was performed on one of the glass specimens to measure the phase response to temperature change near room temperature. The transducer clamping setup was placed within a custom-built environmental chamber with temperature stability of ± 0.01°C over one hour. While holding pressure steady at ~2.8 MPa, the temperature was cycled from 20°C to 25°C and the ultrasonic phase response of the first back-wall reflection was monitored at a driving frequency of 10 MHz.

Ultrasonic measurements for thickness estimation were taken at each of the nine locations on six test specimens. To maintain a consistent couplant thickness, the transducer was loaded with a pressure of ~2.8 MPa each test. Water was used as a couplant for all measurements shown in this work due to its well-known material properties; however, other commercially-available couplants produced similar results. A 6.35 mm diameter, highly-damped, broadband Olympus V112 ultrasonic transducer nominally designed to operate at 10 MHz was used for most measurements, with the exception of some ToF measurements using a 50 MHz transducer.

Using the newly-developed CFPPLL-based ultrasonic phase measurement instrument, the phase of the received wave was tracked as the frequency of the input tone-burst varied from 9 MHz to 10 MHz with a 10 kHz resolution. At each frequency, the phase was averaged over 32 repeated tone-bursts to reduce the effect of noise. The phase vs. frequency response of both the first and second back-wall reflections from the Borofloat specimens were measured.

While still under pressure, the ultrasonic transducer was disconnected from the CFPPLL instrument and connected to a GE Panametrics Model 5900PR Pulser-Receiver to generate and receive broadband pulses for comparative ToF measurements. The generated pulse contained 1 μJ of energy, and the received wave was gained by 40 dB and attenuated by 11 dB. The bandwidth of the generated pulse was chosen to be 1 kHz-200 MHz to make the ultrasonic transducer the bandwidth-limiting element of the system. After amplification, the received echoes from the specimens were displayed on a LeCroy WaveRunner 6200 oscilloscope with 0.1 ns timing resolution. ToF measurements were taken by measuring the difference in time of the peak amplitudes of the first two back-wall reflections and averaging over 500 transmitted pulses.

After the phase and ToF measurements, the 10 MHz ultrasonic transducer was replaced with a 6.35 mm diameter, highly-damped, broadband Olympus V214 ultrasonic transducer designed to operate at 50 MHz. Conventional pulse-echo ToF measurements were obtained with the transducer, similar to the measurements taken with the 10 MHz transducer.

### C. Results and Discussion

Prior to analysis, the effect of couplant reflection was removed by applying a linear fit to the ToF or phase vs. the measured thickness curve. The y-intercept of the line-of-best-fit at zero thickness corresponds to the extrapolated phase or time-delay offset. In total, 4 parameters were extracted from the ToF and phase measurements to predict Borofloat glass thickness: ToF difference between echoes with 10 MHz transducer, ToF difference between echoes with 50 MHz transducer, slope of phase vs. frequency in 9-10 MHz range from first back-wall echo, and slope of phase difference between back-wall echoes vs. frequency in 9-10 MHz range.

#### a.) Correction for Time-Delay and Phase Offsets

FIG. 5 shows plots of two of the time-delay parameters as a function of the specimen thickness. Included in each plot is the line-of-best-fit for the data, which is used to interpolate the time-delay or phase offset at zero specimen thickness. Assuming the couplant thickness and quality is the same for each measurement, the offset measures the phase impact from all sources except for the test specimen. Comparing the phase difference between two consecutive echoes to the phase from the first echo, the phase offset dropped in magnitude, which is consistent with the theory that the phase difference would subtract out some external phase shift sources present in each echo.

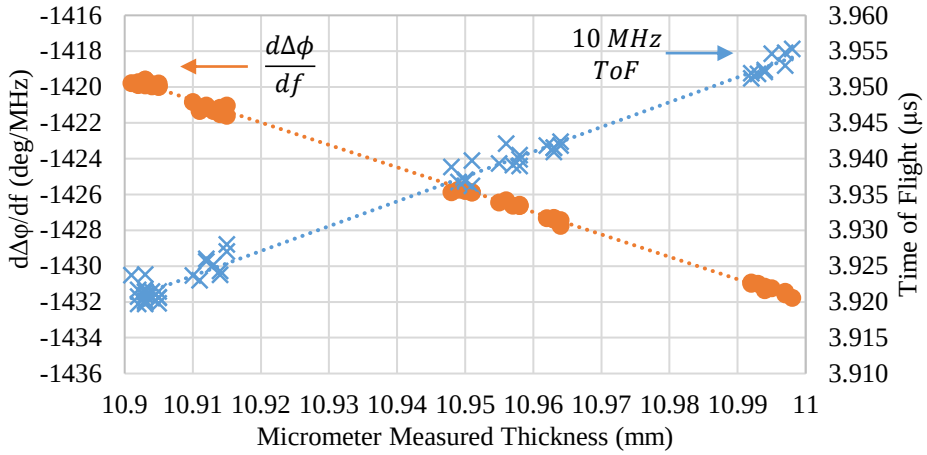


FIG. 5. Time delay parameter vs. thickness for each of the 54 locations, including linear fit for ToF with 10 MHz transducer and $d\,\Delta\,\phi/df$ between consecutive back-wall echoes over 9-10 MHz range

### b.) Glass Thickness from Ultrasonic Measurements

After finding the phase or time-delay offset for each parameter, a thickness for each measurement was calculated from Equations 2 and 3. FIG. 6 shows the difference between the ultrasonically-measured thickness and micrometer measured thickness at each location, for two of the time-delay parameters. Additionally, FIG. 7 shows a box plot of the predicted thickness error from all of the parameters, displaying the median as well as the first and third quartiles of the data. Small plus signs in the box plot represent potential outlier data that fall outside of the quartiles by greater than 1.5 times the interquartile range. Note, $phi\_diff$ is the $\Delta\phi$ phase difference between the first and second back-wall echoes.

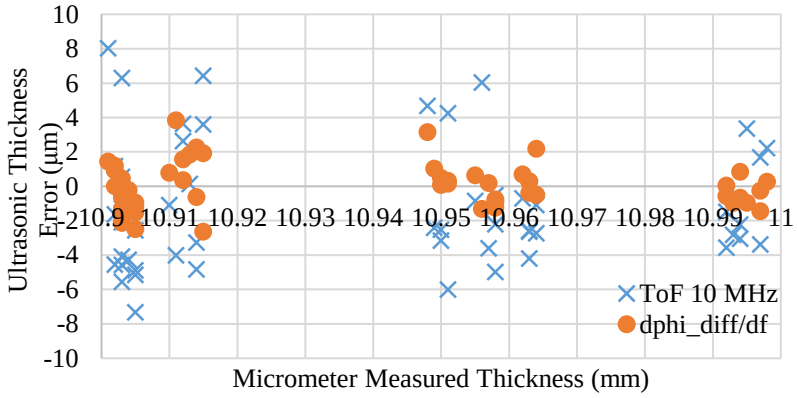


FIG. 6. Difference between ultrasonically measured thickness and micrometer measured thickness for ToF with 10 MHz transducer and dΔϕ/df between consecutive back-wall echoes over 9-10 MHz range

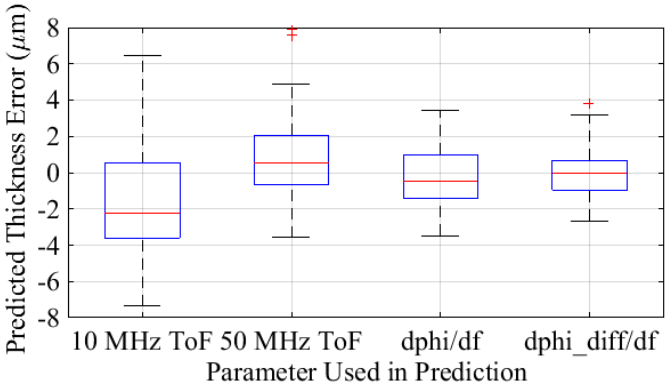

FIG. 7. Box plot of predicted thickness error for each of the 6 time-delay or phase parameters

From comparing predicted thicknesses with measurements with a calibrated micrometer, several conclusions can be drawn. The worst performing parameter tested was ToF measurements with the 10 MHz transducer, with the most significant mean and standard deviation of error. Using the same ultrasonic transducer, the CFPPLL-based ultrasonic measurement parameters performed more accurately and displayed less uncertainty. As predicted, the 50 MHz transducer performed more accurately and precisely than its 10 MHz counterpart. It is thought that the longer pulse duration from the 10 MHz transducer in comparison to the 50 MHz transducer results in higher uncertainty. It is important to note that each of the CFPPLL-based phase parameters performed about the same or better in both accuracy and precision than the ToF measurements from the much higher frequency transducer. Additionally, the phase difference between consecutive echoes resulted in a decrease in the average error and uncertainty for the $d\phi/df$ parameter. This provided the lowest mean error and uncertainty in thickness of all parameters. The $d\Delta\phi/df$ between the first and second back-wall echoes provided a mean predicted thickness error of $-0.04\ \mu m$ and standard deviation of predicted thickness error of $1.35\ \mu m$.

### c.) Sources of Phase Measurement Uncertainty

To improve the accuracy of phase measurements, the sources of uncertainty have been analyzed. Measurements of pressure applied to the transducer and ambient temperature during testing allowed for the impact of these sources of uncertainty to be examined. From an experiment tracking the phase shift due to pressure on the ultrasonic transducer, the phase was found to level off around ~2 MPa, above which $\partial\phi/\partial f$ varied linearly by 0.439 (deg/MHz)/MPa and the phase at 10 MHz varied 3.915 deg/MPa. During thickness gaging experiments, the mean pressure on the transducer was measured to be 2.754 MPa with a standard deviation of 0.031 MPa. Therefore, the phase measurement uncertainty due to applied pressure differences is 0.014 deg/MHz for $d\phi/df$ and 0.112 deg for the phase at 10 MHz.

The phase shift at 10 MHz in the glass specimens due small temperature variations was found to vary linearly 0.715 deg/°C in the 20°C-25°C range, based on testing in an environmental chamber. The mean temperature during ultrasonic thickness gaging tests was measured to be 20.51°C with a standard deviation of 0.18°C. Using the relationship between phase and temperature found in an environmental chamber experiment, the phase measurement uncertainty at 10 MHz due to temperature uncertainty is 0.129 deg.

The standard deviation in phase measurements at 10 MHz is 0.171 deg. Conversion to thickness measurement uncertainty in Borofloat glass via Equation 1 gives a standard deviation of thickness measurement uncertainty of 0.14 μm due to transducer pressure and temperature variations. Combined with the measurement uncertainty of the calibrated micrometer in the 10.9-11.0 mm thickness range, the thickness measurement uncertainty due to the micrometer uncertainty, temperature variations, and transducer pressure variations is 1.06 μm. Thus, most of the 1.35 μm uncertainty using the $d\Delta\phi/df$ phase measurement method is attributed to known sources, the bulk of which is from the micrometer thickness measurements. Comparing the CFPPLL-based ultrasonic phase measurements with a more accurate method or using test specimens with thicknesses known to sub-micron tolerances should improve the predicted thickness uncertainty.

Another potential source of uncertainty is the slight non-linearity of the phase response in the 9-10 MHz range introduced by the reflection off of the couplant layer. Using the slope of the phase vs. frequency response of back-wall reflections depends on the linear relationship between phase and frequency of the test specimen, as described by Equation 1. However, the reflection from the thin couplant layer has an upward concavity, as seen in FIG. 4, and can only be approximated as linear over a sufficiently small frequency range. Consequently, measurement accuracy and uncertainty could be further improved by sweeping over a smaller frequency range.

A final source of uncertainty is inconsistent flatness and parallelism of the test specimens. As seen in the thickness values from FIG. 5, the specimens varied in thickness across their surfaces as much as 14 μm. Thus, the glass specimens do have some inherent lack of flatness or parallelism which contributes to the uncertainties observed. No attempt to correct the phase measurements for flatness and parallelism issues was conducted in this work.

## IV. CONCLUSIONS

A novel single-frequency ultrasonic phase measurement instrument has been built and tested to show its efficacy against conventional ultrasonic time-delay measurement methods. The instrument is digitally-controlled and based on a CFPPLL design, which allows unprecedented ultrasonic phase measurement resolution of to 0.00038 radians (0.022°) or one part in $6.1 \times 10^{-5}$ of an ultrasonic wavelength. Ultrasonic phase can be tracked in real-time for measurement of material property changes due to external stimuli. Unlike previous PPLL-based ultrasonic phase measurement instruments, the system can change driving frequency while also maintaining the previous phase relationship, so swept-frequency phase measurements can be conducted with resolution as low as 3.55 μHz.

Using glass specimens, swept-frequency ultrasonic phase measurements from the CFPPLL instrument were compared with conventional, broadband ToF measurements from a pulser-receiver. After factoring out the time-delay offset due to external sources, the CFPPLL phase measurements outperformed conventional ToF measurements in both accuracy and precision. Furthermore, CFPPLL phase measurements near 10 MHz outperformed much higher frequency 50 MHz ToF measurements. The slope of the phase vs. frequency line taken with the CFPPLL instrument was able to predict thickness with an average error of $-0.04\ \mu m$ and standard deviation of error of $1.35\ \mu m$, which was close to the calibrated micrometer's 1.06 μm uncertainty. Given a

nominal thickness of 10.95 mm, the mean thickness measurement error was -0.00037% of the total thickness and standard deviation of thickness measurement uncertainty was 0.012%.

The newly-developed, digitally-controlled CFPPLL-based phase measurement instrument can provide high-resolution, low-uncertainty ultrasonic time-delay measurements. Its digital control and waveform generation provide major improvements in both resolution and ease-of-use to previous PPLL-based ultrasonic phase measurement instruments. The additional ability to conduct swept-frequency phase measurements will have applications a wide variety of new areas. In addition to improving on conventional ToF methods of sound velocity or thickness measurements in solids or liquids, high-resolution swept-frequency phase measurements may have applicability in areas such as adhesive bond quality assessment, thin film characterization, and ultrasonic analysis of complex structures, such as composites.

## V. ACKNOWLEDGEMENTS

The authors would like to thank Angela Selden and John Callahan for their work in building and testing parts of the CFPPLL instrument. This work was supported by a NASA Space Technology Research Fellowship and the NASA Langley Professor Program.

## VI. REFERENCES

[1] H. J. McSkimin, "Pulse Superposition Method for Measuring Ultrasonic Wave Velocities in Solids," *Journal of the Acoustical Society of America,* vol. 33, no. 1, pp. 12-16, 1961.

[2] E. P. Papadakis, "Ultrasonic Phase Velocity by the Pulse-Echo-Overlap Method Incorporating Diffraction Phase Corrections," *Journal of the Acoustical Society of America,* pp. 1045-1051, 1967.

[3] R. Odru, C. Riou, J. Vacher, P. Deterre, P. Peguin and F. Vanoni, "New instrument for continuous and simultaneous recording of changes in ultrasonic attenuation and velocity," *Review of Scientific Instruments,* vol. 49, no. 2, pp. 238-241, 1978.

[4] S. Taki, Y. Furuta and T. Takemura, "New Instrument for Rapid Measurement of Changes in Ultrasonic Velocity," *Review of Scientific Instruments,* vol. 52, no. 9, pp. 1388-1391, 1981.

[5] T. Pialucha and P. Cawley, "The Detection of Thin Embedded Layers using Normal Incidence Ultrasound," *Ultrasonics,* vol. 32, no. 6, pp. 431-440, 1994.

[6] A. I. Lavrentyev and S. I. Rokhlin, "Determination of Elastic Moduli, Density, Attenuation, and Thickness of a Layer using Ultrasonic Spectroscopy at Two Angles," *Journal of the Acoustical Society of America,* vol. 102, no. 6, pp. 3467-6477, 1997.

[7] C. Jin, "A Continuous Wave Method for Simultaneous Sound Velocity and Attenuation Measurements," *Review of Scientific Instruments,* vol. 67, no. 1, pp. 271-273, 1996.

[8] R. J. Blume, "Instrument for the Dontinuous and High Resolution Measurement of Changes in the Velocity of Ultrasound," *Review of Scientific Instruments,* vol. 34, no. 12, pp. 1400-1407, 1963.

[9] J. S. Heyman and E. J. Chern, "Ultrasonic Measurement of Axial Stress," *ASTM Journal of Testing and Evaluation,* vol. 10, no. 5, pp. 202-211, 1982.

[10] W. T. Yost, J. H. Cantrell and P. W. Kushnick, "Fundamental aspects of pulse phase-locked loop technology-based methods for measurement of ultrasonic velocity," *Journal of the Acoustical Society of America,* vol. 91, no. 3, pp. 1456-1468, 1992.

[11] W. T. Yost, J. H. Cantrell and P. W. Kushnick, "Constant Frequency Pulsed Phase-Locked-Loop Instrument for Measurement of Ultrasonic Velocity," *Review of Scientific Instruments,* vol. 62, no. 10, pp. 2451-2456, 1991.

[12] V. N. Bindal, "Water-Based Couplants for General Purpose Use for Ultrasonic NDT Applications," *Journal of Scientific and Industrial Research,* vol. 59, pp. 935-939, 2000.

[13] M. Redwood and J. Lamb, "On the Measurement of Attenuation in Ultrasonic Delay Lines," *Proceedings of the IEEE: Radio and Electronic Engineering,* vol. 103, no. 12, pp. 773-780, 1956.

[14] T. Inamura, "The Effect of Bonding Materials on the Characteristics of Ultrasonic Delay Lines with Piezoelectric Transducers," *Japanese Journal of Applied Physics,* vol. 9, no. 3, pp. 255-259, 1970.

[15] Y. H. Kim, S.-J. Song, S.-S. Lee, J.-K. Lee, S.-S. Hong and H. S. Eom, "A Study on the Couplant Effects on Contact Ultrasonic Testing," *Journal of the Korean Society for Nondestructive Testing,* vol. 22, no. 6, pp. 621-626, 2002.

[16] A. Vincent, "Influence of Wearplate and Coupling Layer Thickness on Ultrasonic Velocity Measurement," *Ultrasonics,* vol. 25, pp. 237-243, 1987.

[17] T. Reddyhoff, S. Kasolang, R. S. Dwyer-Joyce and B. W. Drinkwater, "The Phase Shift of an Ultrasonic Pulse at an Oil Layer and Determination of Film Thickness," *Proceedings of the Institution of Mechanical Engineers, Part J: Journal of Engineering Tribology,* vol. 219, no. 6, pp. 387-400, 2005.